Research Article

Microcapsules responsive to pH and temperature: synthesis, encapsulation and release study

Nagaraju Pentela[1,2] · Simran Rainu[1] · N. Duraipandy[2,3] · A. A. Boopathi[1,2] · M. S. Kiran[3] · Srinivasan Sampath[4] · Debasis Samanta[1,2]

Abstract
In this present article, we report preparation of dual responsive microcapsules by using poly(*N*-isopropyl acrylamide-co-methacrylic acid) [poly(NIPAM-co-MAA)] and acid functionalized graphene oxide (GO). While the methacrylic acid part is responsible for the responsiveness towards the change in pH, *N*-isopropylacrylamide part is responsible for the responsiveness towards change in temperatures. Functionalized GO forms the core of the microcapsules and its interaction with the polymer controls the movement of the encapsulated materials in response to change in neighboring environment. Surface morphology and interconnectivity of the microcapsules was observed by optical polarized microscopy and the presence of the GO sheets on the wall was observed in High Resolution Transmission Electron Microscopy images. The pH and temperature responsive nature of the microcapsules were studied by loading vitamin B2 or anticancer drug cisplatin. It was found that both pH and temperature influences releasing pattern of the either drug from microcapsule.

Keywords Graphene oxide · Thermoresponsive · pH responsive · Polymers · Drug delivery

1 Introduction

The stimuli responsive microcapsules [1] have drawn attention recently because it can be conveniently used to trigger the controlled release of drug molecules at a specific site of the body by using the surrounding stimuli such as temperature, pH, light, and ultrasound etc [2–5]. For example, Gao et al. [4]reported stimuli responsive multifunctional microcapsules with high mechanical stability to release the encapsulated materials triggered by UV and Ultrasound. Gold nanoparticle-based polyelectrolyte microcapsules can trigger the release of the encapsulated materials by Near Infrared (NIR) irradiation (1064 nm) as reported by Angelatos et al. [6] In those cases, the trigger release was caused by an external light source that may damage the normal cells while placing under strong light source. Bi et al. [7] prepared another kind of microcapsules responsive by a magnetic field. Li et al. [8] recently reported a dual responsive (magnetic and redox-responsive) folic acid functionalized microcapsules as hydrophobic drug carriers. Along the same line, Yujie Ma et al. [9] reported poly (ferrocenylsilane)-based microcapsules, responsive towards the change in redox potential. Dong et al. [10] recently reported dual responsive microcapsules based on magnetic stimuli. However, the encapsulation of the drug either under the strong magnetic field or in the presence of metal nanoparticles and redox conditions may change the texture and sensitivity of the microcapsules.

Electronic supplementary material The online version of this article (https://doi.org/10.1007/s42452-019-0371-1) contains supplementary material, which is available to authorized users.

✉ Debasis Samanta, debasis@clri.res.in; Srinivasan Sampath, srinivasansampath@cutn.ac.in | [1]Polymer Science and Technology Department, Council of Scientific and Industrial Research (CSIR)-CLRI, Adyar, Chennai 600020, India. [2]Academy of Scientific and Innovative Research, Rafi Marg, New Delhi, India. [3]Biological Material Laboratory, CSIR-CLRI, Chennai 600020, India. [4]Department of Materials Science, School of Technology, Central University of Tamil Nadu, Thiruvarur 610101, India.

SN Applied Sciences (2019) 1:448 | https://doi.org/10.1007/s42452-019-0371-1

Received: 2 October 2018 / Accepted: 18 March 2019 / Published online: 11 April 2019

To address those concerns, Zeng et al. [11] reported multi stimuli responsive microcapsules made of biodegradable polymeric nanoparticles that improved the trigger release of active fluorescence drug, doxorubicin, in acidic medium and at higher temperatures. Stable pH responsive microcapsule was fabricated by using functionalized carbon nanotube and ytterbium triflate for controlled drug delivery. Zhang et al. [12] reported polymeric membranes with dual responsive properties which had been used for the encapsulation of the proteins and peptides. Further, dual-stimuli responsive polymers, sensitive to varying temperatures and pH, find potential applications in cancer treatment. The tumor cells are known to have lower pH and significantly higher temperature than normal tissue cells. Therefore, pH-temperature dual stimuli responsive polymer based microcapsules can be used as a carrier of the anticancer drug to release at the specific site triggered by lower pH and higher temperature. In this context, use of the suitable polymer (for responsiveness) and proper carbon material (to construct the robust skeleton of the microcapsules) should provide a direction towards designer microcapsules whose release mechanism can be tuned against temperature and pH simultaneously. *N*-isopropylacrylamide based polymers can provide the responsiveness to temperature changes while methacrylic acid-based polymers can provide responsiveness towards pH change. For example, Poly(NIPAM) based thermoresponsive polymers were prepared for hydrogel formation [13] or for catalyst recovery [14]. On the other hand pH responsive polymers were prepared and used extensively for drug delivery applications [15].

Here in this study, we prepared dual responsive microcapsules (temperature and pH) using a copolymer comprising of both acid and temperature sensitive groups and carbon nanomaterials with the suitable functional group. Notably, we used poly(NIPAM-co-MAA) polymer, which was prepared from monomers N-isopropylacrylamide and methacrylic acid by free radical polymerization method (Fig. 1a). The stable (Fig. 1b) microcapsules were prepared from this polymer and acid functionalized graphene oxide. The graphene oxide was chosen because of its flat sheet-like structure, to provide stability to the walls of the microcapsules [16, 17]. Particularly, it can prevent uncontrolled leakage of the encapsulated materials [18] to improve the specific responsiveness during the release process. Further, functionalization of graphenes induces various noncovalent interactions (Fig. 1c) between the polymer and graphene oxide [18] for the improved stability of the microcapsules. To the best of our knowledge, this is the first report of preparation of dual responsive microcapsules from functionalized graphene oxide which can be conveniently used for loading of riboflavin to study the responsiveness by both pH and temperatures. Further, the fabricated microcapsules are well-defined and interconnected in many cases (Fig. 1d) due to

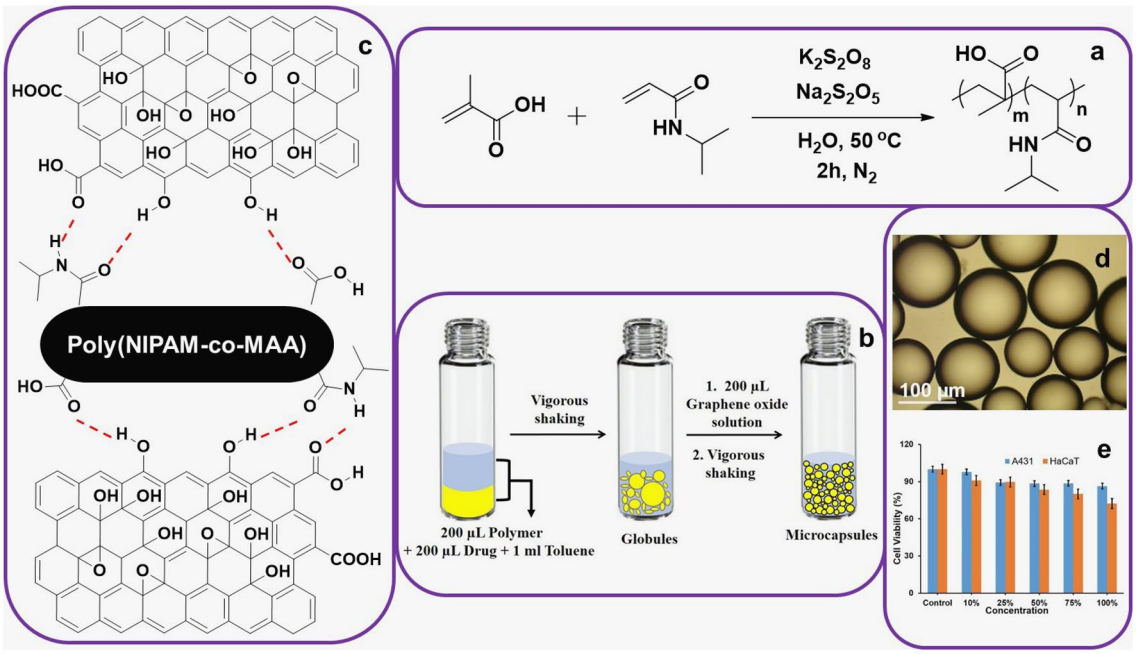

Fig. 1 **a** Schematic representation of the synthesis of Poly(*N*-isopropylacrylamide-co-methacrylic acid) [Poly(NIPAM-co-MAA)] polymer by free radical polymerization. **b** Schematic representation of microcapsules formation. **c** Schematic representation of different possible non-covalent interactions/bonding between the nanomaterial and polymer in microcapsules. **d** Optical microscopic images of well-interconnected microcapsules. **e** Cell viability of the synthesized polymer solution

strong non-covalent interactions. Those interconnection can provide additional protection from mechanical disturbance to prevent undesired release of the materials from the microcapsules [19, 20] The synthesized copolymer along with functional graphene oxide of the [21] specific amount is found to be biocompatible (Fig. 1e) and useful for the microcapsules preparation where the microcapsules can be used as a drug carrier for drug delivery applications.

2 Experimental

2.1 Materials and instrumentations

N-isopropylacrylamide, Methacrylic acid, Riboflavin (Vitamin B2), Cisplatin [cis-diaminedichloroplatinum(II)], Deuterium oxide were purchased from Sigma Aldrich and used without further purification. Toluene, Hexane, Potassium persulphate, Sodium metabisulphite (from Merck India) were used as received. ^{1}H NMR (Proton Nuclear Magnetic Resonance) spectroscopy was done at 400 MHz using Bruker Avance-III spectrometer. Fourier-transform infrared spectroscopy (FT-IR) was done using JASCO FT/IR-4200. TGA analysis was performed by using Q50, TA instrument with a heating rate 10 °C/min under N_2 atmosphere. DSC experiments were performed by using Netzsch DSC 214 Polyma with a heating rate of 10 °C/min under N_2 atmosphere. Raman experiment was performed by using LabRAM HR Evolution Raman Spectrometer. Dynamic Light Scattering analysis (DLS) was carried by using ZETASIZER Nano-ZS, model ZEN3600. Field Emission Scanning Electron Microscopy (FESEM) experiments were carried out using Zeiss ultra-55. HR-TEM experiments were performed using FEI Technai G^2 S-Twin; the operating accelerating voltage was 200 kV. Optical Polarized Microscope (OPM) images and videos were captured by using the OLYMPUS BX50 microscope. Fluorescence microscopic images were captured by LEICA DMIRB microscope. Atomic absorption spectroscopy (AAS) was carried out by using AAS, NovAA 350-Analytik Jena, Germany. Fluorescence spectroscopy was carried out using VARIAN CARY Eclipse Fluorescence Spectrophotometer. Fluorescence images were taken in near UV region in the range of 200 nm to 400 nm. All the solutions were prepared using distilled water. Sodium acetate buffer solutions were used for responsive study and washing of microcapsules.

2.2 Synthesis of poly(*N*-isopropylacrylamide-co-Methacrylic acid) [Poly(NIPAM-co-MAA)]

The copolymer was synthesized by radical polymerization using a combination of persulphate-metabisulphite catalyst which can initiate the polymerization at a slightly elevated temperature [22]. This type of polymerization was chosen because of reproducibility and convenience in scaling up to a higher scale [23]. The procedure was slightly modified to retain the dual responsive characteristics. The procedure of polymerization is described below.

In a two-neck, 100 ml round bottom flask, (500 mg, 4.41 mmol) NIPAM was dissolved in 10 ml of distilled water. To this, solutions of potassium persulphate (100 mg, 0.36 mmol in 5 ml of distilled water) and sodium metabisulphite (10 mg, 0.05 mmol in 5 ml of distilled water) were added. The reaction mixture was stirred for 5-10 min followed by the addition of (250 mg, 2.90 mmol) methacrylic acid. The stirring was continued for 2 h under N_2 at 50 °C. The solution becomes turbid within 5 min, after 2 h a white precipitation was observed. 20 ml distilled water was added to the reaction mixture and it was kept overnight. The precipitate was filtered in hot condition and washed twice with hot distilled water. The polymer was vacuum dried and analyzed by ^{1}H NMR, IR, TGA and DSC.

2.3 Synthesis of graphene oxide (GO)

Graphene oxide was prepared from graphite by following our previous literature report using modified Hummers method. [24–28] It has a morphology of a planner sheet with a few functional groups like hydroxyl and carboxylic acid groups which can participate in non-covalent interactions with other materials like polymers and nanoparticles.

2.4 Poly(NIPAM-co-MAA)/GO based microcapsules with encapsulated materials

200 µL of poly *N*-isopropyl acrylamide-co-Methacrylic acid solution [Poly(NIPAM-co-MAA)] (5 mg in 1.5 ml of distilled water), 200 µL riboflavin solution (1 mg/mL of distilled water) or cisplatin (9.48 mg in 4 ml of pH 7 sodium acetate buffer solution) and 1 mL toluene were stirred in a 7 mL sample vial for a minute. To this, 200 µL of GO solution (1 mg/mL of distilled water) was added and stirred vigorously for a minute to obtain microcapsules. The microcapsules were washed twice with 1 mL of hexane and then with 1 mL of sodium acetate buffer solution (pH 7). The sample vial was kept open for about several hours to evaporate excess of hexane.

2.5 Study of Drug Release from Microcapsules at Different pH and Temperatures

After forming the microcapsules with encapsulated materials, they were placed under the buffer solutions at a specific pH and temperatures to study the release dynamics. Microcapsules were prepared freshly each time before placing it in a buffer of specific pH and temperature. For examples, microcapsule with encapsulated riboflavin

was placed in a buffer of pH 4 at 30 and 40 °C separately. This experiment was repeated at pH 7. The results were presented in Figs. 4 and Fig. 5b. To further confirm the pH-responsiveness at lower pH variation, another set of experiments were conducted in a similar fashion at 32 °C, in the buffers of pH 4 and 7 and the results were presented in Fig. 5.

3 Results and discussion

3.1 Optical microscopic studies of microcapsules

Several batches of microcapsules were prepared to study the effect of pH and temperature on the morphology and stability of the microcapsules. Several images and videos were recorded, it was noticed that the microcapsules were interconnected and showed stability towards the mechanical disturbance (blow of N_2 gas onto the microcapsules) (Movie in ESI- nitrogen blow between 4 and 5 s).

In this case, the functionalized graphene sheets directly interacted with the copolymer through multiple non-covalent interactions. The amide and carboxylic acid functional groups present in the [Poly(NIPAM-co-MAA)] form H-bonding with various functional groups attached with graphene as shown in Fig. 1c. In the absence of the graphene, the microcapsules are not stable. The supramolecular interaction between them results in the stable micro-capsule formation.

The white color highlighted arrows from Fig. 2a (at 30 °C) and Fig. 2b (at 38 °C) represents the change in diameter of the microcapsules with temperature. We observed that with an increase in temperature there was a decrease in diameter (Fig. 2b white arrows) of the microcapsules which may lead to increase in the internal pressure which will be useful to release the drug from microcapsules at high temperature. We also carried out a control experiment by using polymethacrylic acid microcapsules at the same temperature conditions (from ESI Figure.S1). In that case the diameter of the microcapsules was not affected by the changing temperatures. This indicated the usefulness of the microcapsules for temperature dependent release study.

3.2 Electron microscope study

The microcapsules were drop casted onto the aluminum foil for FESEM, and on the copper grid for HRTEM. The images were taken in high magnification of a part of microcapsules to understand the morphology of the microcapsules and the influence of the nanomaterials. As shown in Fig. 3a the wrinkles and agglomeration of the polymer around graphene sheets may cause surface roughness at pH 7.5 whereas in lower acidic pH 5.2 (Fig. 3b) higher/large pore sizes (white highlighted arrows) were observed possibly because of weaker non-covalent interactions between the nanomaterials and polymers at lower pH. In transmission electron microscopy, well-spread polymer on graphene sheet was observed under pH 7.5 (Fig. 3c) whereas in lower acidic pH 5.2 (Fig. 3d) the polymer layers were stacked as multiple sheets. The largely intact graphene sheets indicate its robustness in preparing the skeleton of stable microcapsules.

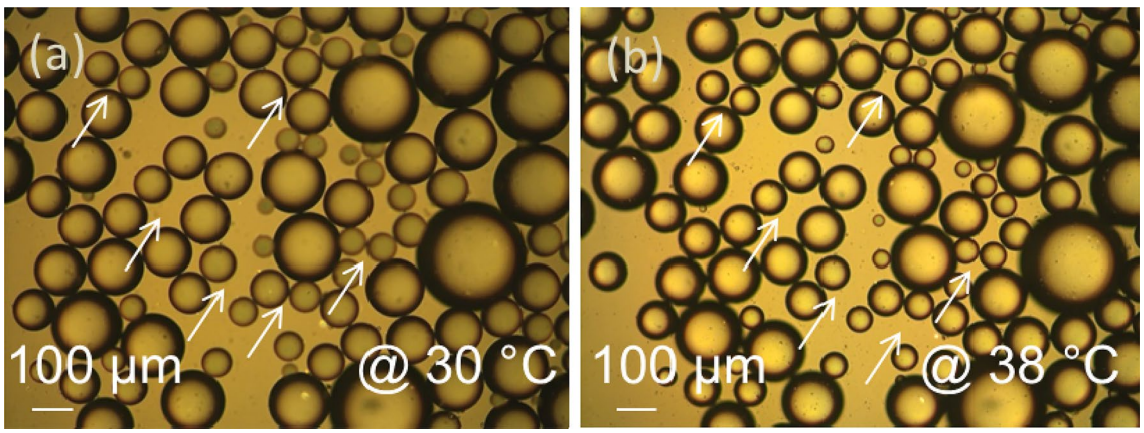

Fig. 2 **a** OPM images of [Poly(NIPAM-co-MAA)]/GO microcapsules at 30 °C **b** OPM images of [Poly(NIPAM-co-MAA)]/GO microcapsules at 38 °C. The microcapsules marked with white arrow shrunk after heating, due to the presence of temperature responsive polymeric part. Temperature-dependent release of the encapsulated materials may be attributed to this phenomenon of shrinkage by heating

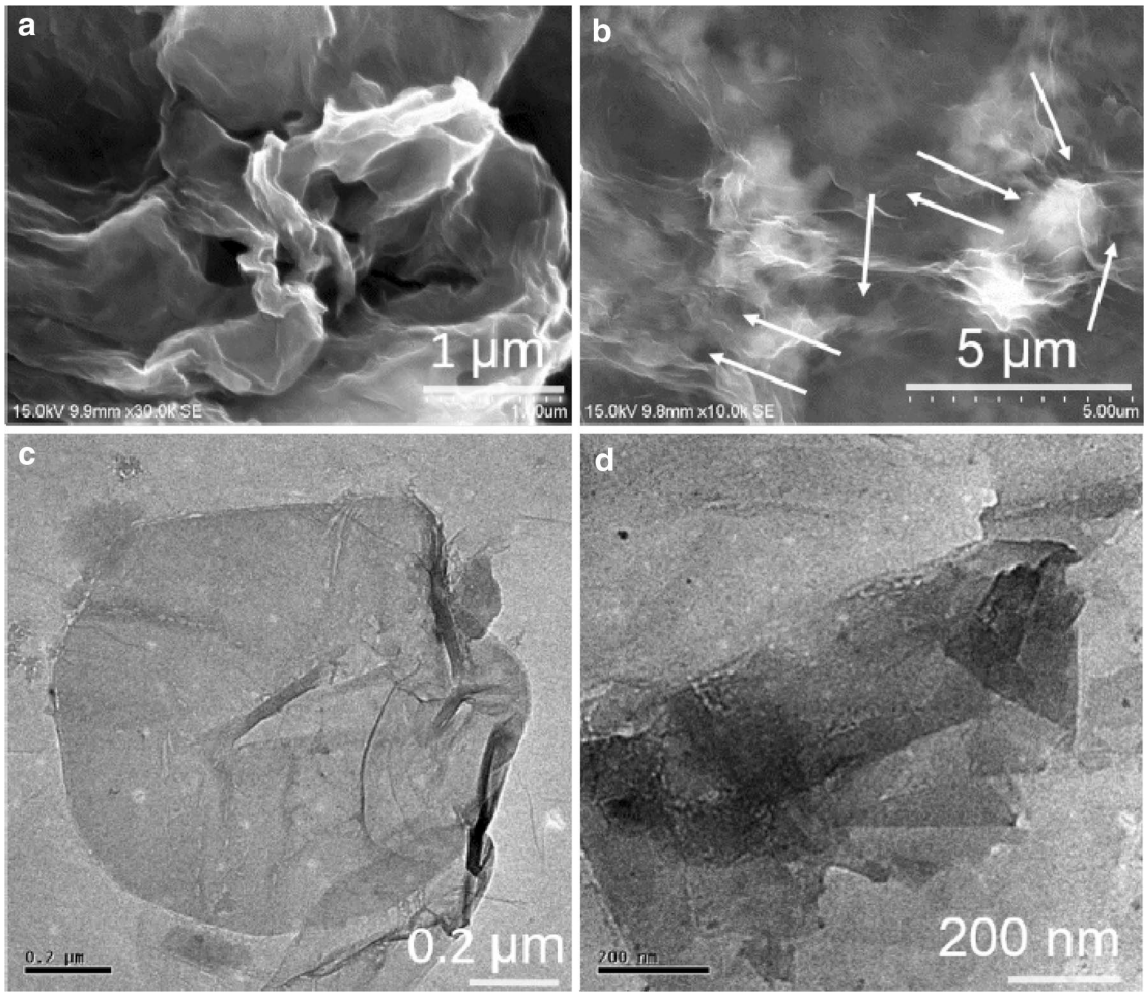

Fig. 3 FESEM images of microcapsule at **a** pH 7.5 **b** pH 5.2. The white arrows on the microcapsules at lower pH indicated a number of holes which should be responsible for transportation of encapsulated materials; HRTEM images of dried microcapsules at **c** pH 7.5 **d** pH 5.2. Crumbled largely intact graphene sheets were observed in both the cases

3.3 Study of drug release from microcapsules at various pH and temperatures by UV illumination

To analyze the release behaviour of microcapsules, the microcapsules were kept at different pH and temperature in different sample vials. 200 µL of sample solution was collected in eppendorf at one hour time interval. These samples were then illuminated by UV light. The release of drug was faster and more in pH 4 (Fig. 4a) as compared to pH 7 (Fig. 4c). Similarly, the release of the drug was faster in pH 4 (Fig. 4b) than compared to pH 7 (Fig. 4d) indicating that the fabricated microcapsules are pH responsive. As observed from the UV illumination images for thermoresponsive drug release from microcapsules, the release of drug was higher at 40 °C (Fig. 4b, d) as compared to 30 °C (Fig. 4a, c).

In pH 7, at 30 °C the drug release could be observed prominently after the 18th hour (Fig. 4c) whereas at 40 °C the release could be observed after the 2nd hour (Fig. 4d) itself under same pH conditions. Additionally, the drug release concentration was more prominent from 5th hour (Fig. 4b) at 40 °C as compared to the 23rd hour (Fig. 4a) at 30 °C under pH 4. The higher release of drug at 40 °C is possibly due to phase separation (as shown in DSC, ESI Figure. S2) above 35 °C when the breakage of the hydrogen bonding may lead to the higher drug release concentration.

3.4 Study of drug release from microcapsules at various pH and temperature by fluorescence spectroscopy

The pH and temperature dependent release behaviour of riboflavin from microcapsules was studied by fluorescence

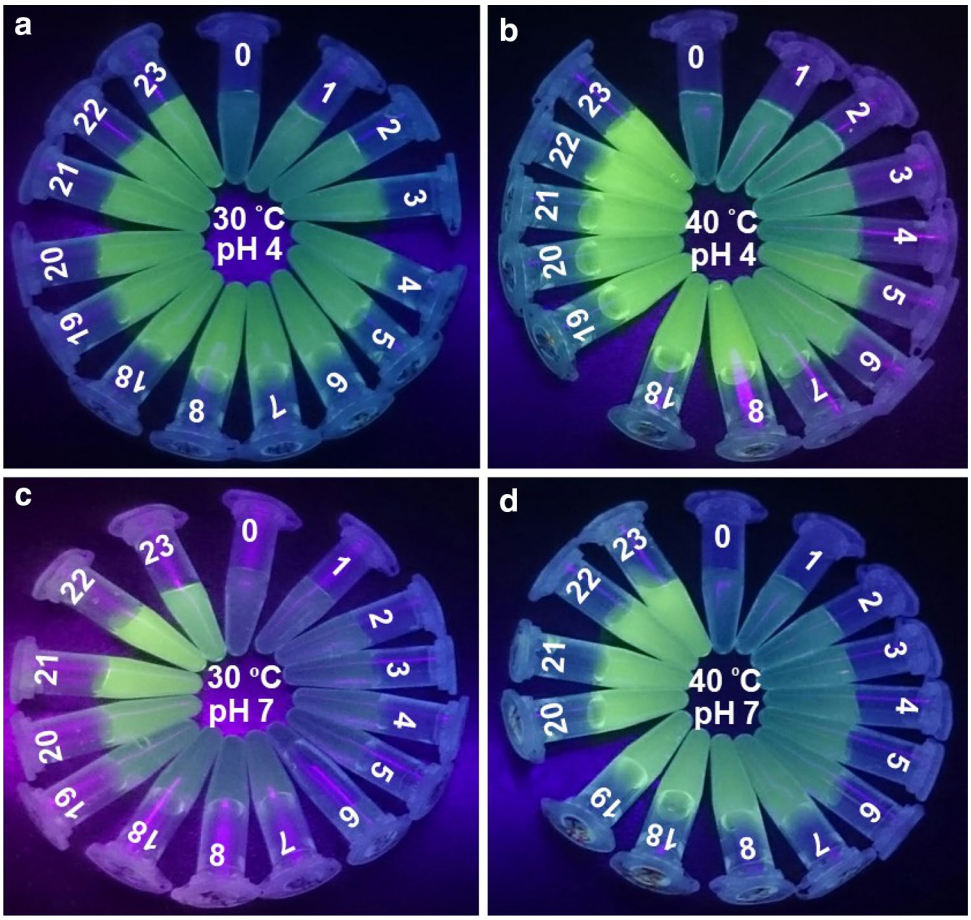

Fig. 4 pH and temperature dependent (**a**–**d**) drug release study under UV light illumination. The samples were collected in eppendorf every 1 h interval and are arranged in a clockwise manner with increasing time. Image **a** at 30 °C and **b** at 40 °C in pH 4; image **c** at 30 °C and **d** at 40 °C in pH 7

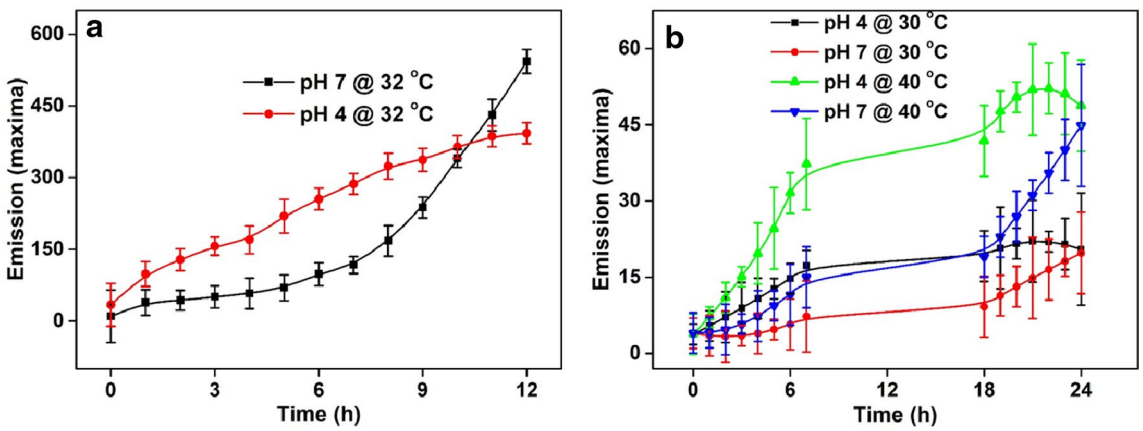

Fig. 5 Study of the release of riboflavin from microcapsules at different pH and temperature by fluorescence spectroscopic technique (the excited and emission wavelengths are at 440 nm and 525 nm respectively). **a** Release at different pH under a constant temperature of 32 °C **b** release at different temperature and pH. The release was more at lower pH and higher temperature

spectrophotometer (Fig. 5). In all cases, general trends of initial higher release efficiency (up to 10 h) at lower pH and higher temperature (Fig. 5b, green curve) were observed. A reaching of saturation point in the drug release profile was observed more quickly when microcapsules were placed at lower pH and higher temperature (Fig. 5b). While temperature dependent release efficiency may be attributed to shrinking of NIPAM part of polymers due to the breaking of hydrogen bonding at a higher temperature and the pH-dependent release efficiency may be attributed to the variation of charge of the polymer at different pH.

This was further confirmed by DLS (Dynamic Light Scattering) study, which showed the polymer has higher net negative charge under neutral pH 7 (ESI Figure.S3) than acidic pH 4 (ESI Figure.S4). Due to this high net negative charge at neutral pH, the polymer may bind strongly to GO sheets leading to higher stability of the microcapsules and thus slower release of drug at neutral pH than lower acidic pH.

3.5 Study of the release of the anticancer drug cisplatin by atomic absorption spectroscopy (AAS)

We carried out AAS studies using the anticancer drug cisplatin. The pH dependent cisplatin release study indicated that the release was higher at pH 4 (Fig. 6a, red curve). The released concentration of the cisplatin at 21st hour is 5 ppm in pH 4 which was double than that of 2 ppm at 21st hour at pH 7. The temperature responsive release study indicated that the release was more at 40 °C (Fig. 6b, pink curve) in pH 4 than at 40 °C in pH 7 (Fig. 6b, blue curve). Moreover, the release concentration of cisplatin at 40 °C was more than the release concentration of cisplatin in lower pH 4 (Fig. 6b, red curve) or higher pH 7(Fig. 6b, black curve) at 30 °C.

3.6 Study of drug release from microcapsules at various pH by fluorescence microscopy

Since riboflavin is fluorescence active, it is useful to study the release efficacy by fluorescence microscope at different pH. As observed from Fig. 7a, almost none of the microcapsules have fluorescence on it, since most of the riboflavin is still encapsulated inside at pH 7. As observed from Fig. 7b, slight fluorescence stains were observed on several microcapsules after a minute in pH 4. This can be attributed to a small release of flurorescent riboflavin at lower pH within a short period of time. It was also visible while using different filters in fluorescence microscope studies (ESI Figure.S5).

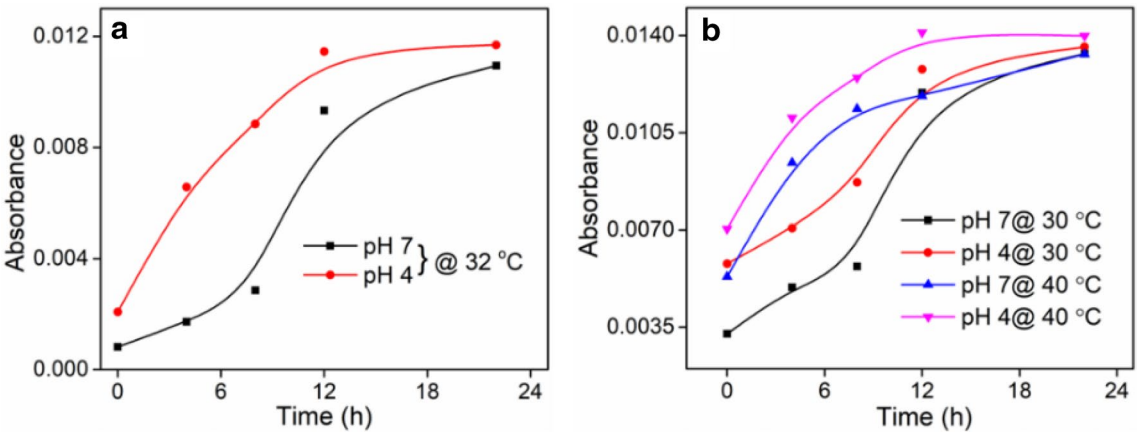

Fig. 6 **a** AAS absorbance versus time graph corresponds to pH dependent release study **b** corresponds to temperature dependent release study. **a** red curve at pH 4, the black curve at pH 7 @ 32 °C. **b** Black curve at pH 7 @ 30 °C, red curve at pH 4 @ 30 °C, blue curve at pH 7@ 40 °C, pink curve at pH 4 @ 40 °C

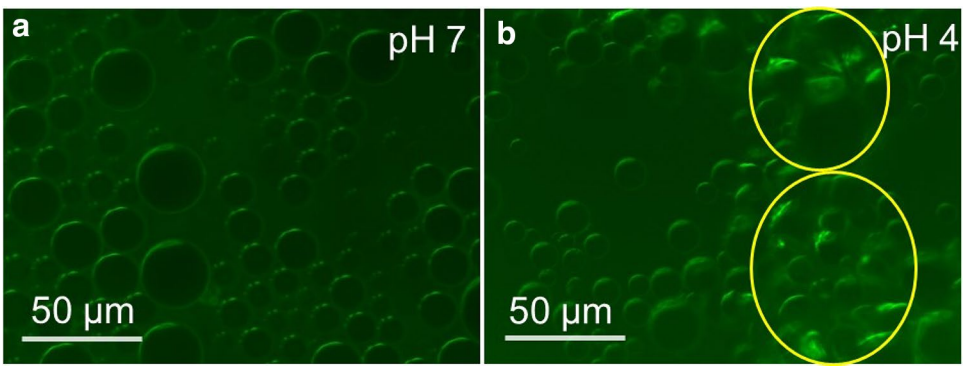

Fig. 7 Fluorescence images of riboflavin encapsulated microcapsules in surrounding medium after placing it under buffers of different pH; **a** after placing the microcapsules under pH 7 and **b** after placing the microcapsules at pH 4. The area under yellow highlighted circles (right side image) shows the release of the encapsulated riboflavin glowed by fluorescence after 1 min

3.7 Cytotoxicity study of the polymer solution

Cytotoxic effect of synthesized polymer was assessed by MTT Assay. Briefly, HaCaT (immortalized human keratinocytes) cells were seeded to grow for 24 h at 37 °C in a 5% CO_2 and 95% O_2 humidified incubator. Once the cells had its morphology, the cells were treated with varying concentrations of polymer solutions like 10%, 25%, 50%, 75%, and 100% was incubated at 37 °C for 24 h. After incubation, 0.5 mg/ml of MTT (Thiazolyl Blue Tetrazolium Bromide salt) in 1X PBS (500µL/well) was added and kept it for 4 h in dark/ 37 °C. The MTT assay was carried out in triplicates. Following 4 h incubation with MTT solution, the MTT solution was removed, and formazan crystal was solubilised with 200µL DMSO and the absorbance at 570 nm was measured using BioRad ELISA plate reader. The percentage of cell viability was calculated by the following formula.

$$\text{Cell Viability}\,(\%) = (\text{O.D of treated cells}/\text{O.D of untreated cells}) * 100\,(\text{O.D } s\tan ds \text{ for optical density}).$$

The biocompatibility of the solution of all constituents of microcapsules is shown in Fig. 8. The solution shows more than 80% cell viability up to 1.8%.

The results indicated that the [Poly (NIPAM-co-MAA)] polymer did not exhibit any cyto-toxicity in both normal keratinocyte HaCaT cell line and cancerous keratinocytes A431cell line. The result indicated that the polymer solution does not induce any cytotoxicity in both normal and cancerous cell line at concentration even as high as 1.8%. The results are consistent with ISO standard (ISO 10993 Part 5) where cell viability above 70% when compared to control cells is considered acceptable as non-cytotoxic. The result indicated that the polymer remain as inert material without any toxicity towards the any cell type. Hence the polymer is a suitable material for microcapsules preparation for the delivery of anti-cancer drugs in a site specific manner.

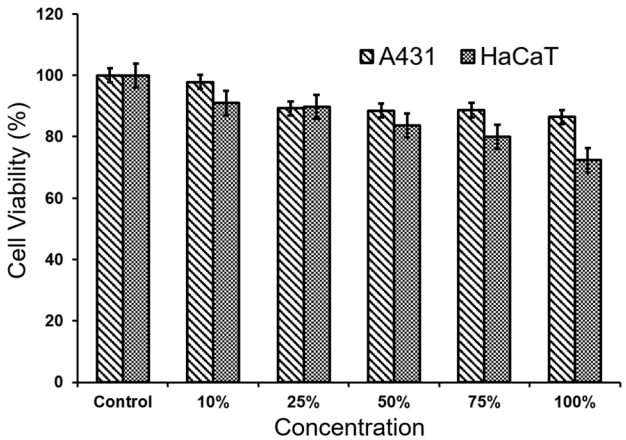

Fig. 8 MTT assay of the [Poly(NIPAM-co-MAA)] polymer along with the other constituents of microcapsules

3.7.1 ^{1}H NMR analysis

Success of the polymerization was confirmed by ^{1}H NMR spectroscopy. The complete disappearance of monomer peaks around 5–6 ppm and appearance of a broad peak in between 0.80 to 1.97 ppm (ESI Figure.S6) indicated the success of polymerization.

3.8 FT-IR spectroscopy

FTIR spectroscopy was used to understand the presence, states of functional groups of different materials and their various interactions. As shown in ESI Figure. S7 black curve, the polymer shows peaks at 3428 cm^{-1} for –(OH_{str}) of carboxylic acid, 2997 cm^{-1} for –(CH_{str}), 1711 cm^{-1} for carbonyl –($C{=}O_{str}$) of methacrylic acid, 1638 cm^{-1} for –($C{=}O_{str}$) of amide, 1545 cm^{-1} for –(NH_{ben}) of amide group and 1168 cm^{-1} for –($C{-}O_{str}$). As observed in ESI Figure. S7 red curve, peak at 3466 cm^{-1} corresponds to the –(OH_{str}) and 1638 cm^{-1} corresponds to –($C{=}O_{str}$) of the carbonyl group of acid functionalized graphene oxide was assigned. The disappearance of the peak at 1711 cm^{-1} and a decrease in the peak intensity at 1638 cm^{-1} (in Figure. S7 blue curve) may be attributed to the formation of the noncovalent interactions between the copolymer and functionalized GO.

3.9 Thermal study

(a) TGA analysis

The thermal stability studies were carried out by using Thermogravimetric Analysis (Fig. 9).

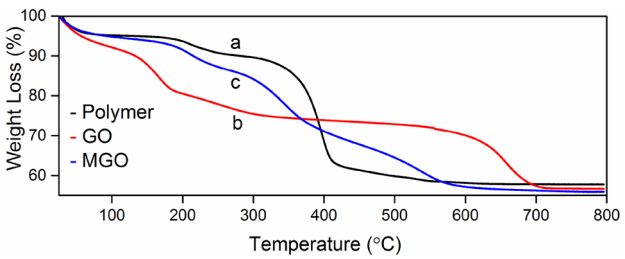

Fig. 9 TGA analysis of **a** poly(NIPAM-co-MAA) **b** graphene oxide **c** poly(NIPAM-co-MAA)/GO microcapsules (dried powder). An increase in the stability after microcapsule formation is plausibly facilitated by several non-covalent interactions

As shown in Fig. 9a, three main degradation temperature were observed for the polymer, the first and second degradation temperature was observed at 200 °C and 336 °C with a weight loss of 14%, and 13% respectively. The final degradation temperature was observed at 430 °C with a weight loss of 57%. As evident from Fig. 9b, the maximum weight loss (19%) of GO was observed at around 189 °C can be attributed by the decomposition of labile oxygen-containing functional groups. As observed from Fig. 9c, the maximum weight loss (33%) of MGO was observed at around 483 °C possibly by the noncovalent attachment of polymer chains on GO sheets. Hence, it was evident that the prepared microcapsules are more stable than parent polymer. It may be attributed to several noncovalent interactions between polymer and nanomaterials.

(b) DSC analysis

DSC was used to measure the glass transition Temperature (T_g) and temperature responsiveness in water of the copolymer. As shown in Fig. 10, the glass transition temperature of the polymer was observed in 171 °C which is usual for a NIPAM-based copolymer [29].Interestingly, we also observed cloud point temperature at 35.1 °C (ESI Figure. S2). For this 10 mg of Poly(NIPAM-co-MAA) was dissolved in 1 ml of pH 7 buffer solution and DSC was performed from 0 to 50 °C with a heating rate 10 °C/min under N_2 atmosphere. This kind of cloud point temperature of polymeric materials was observed by Zhang [30] and Schonhoff [31] et al.

3.10 Raman analysis study

The characteristic D and G bands of GO at 1346 cm^{-1} and 1582 cm^{-1} respectively are observed in the Raman spectra given above (Fig. 11b). A shift in the characteristic D and G bands towards higher values at 1357 cm^{-1} and 1598 cm^{-1} respectively have been observed in the case of MGO (Fig. 11a). This shift to higher values may be attributed to non-covalent interactions between the polymer and functionalized Graphene oxide.

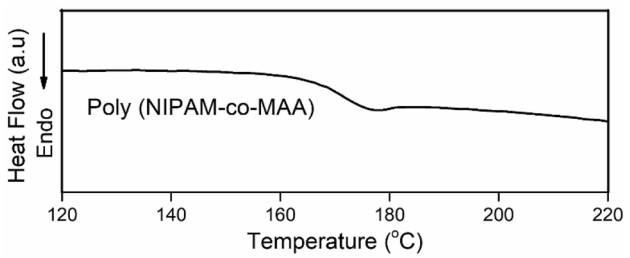

Fig. 10 DSC thermogram of poly(NIPAM-co-MAA) showed a glass transition at a temperature of 171 °C

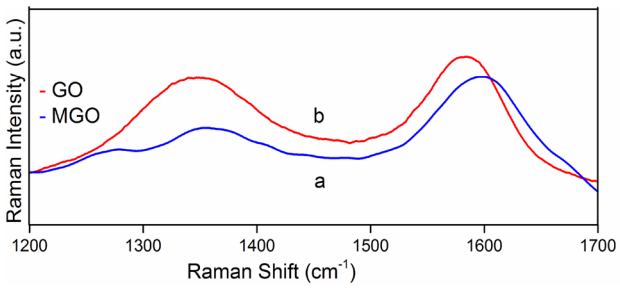

Fig. 11 **a** Raman Spectrum of microcapsules Graphene oxide (MGO). **b** Graphene oxide (GO) was obtained by irradiating the samples with 576 nm laser beam. Samples were prepared by spraying the solid (powder) form of GO and MGO uniformly on the glass slide

4 Conclusion

In conclusion, we reported a novel and convenient method for the preparation of dual responsive polymer/graphene oxide based microcapsules. The microcapsules were highly stable in the presence of graphene oxide, and the possible noncovalent interactions between [Poly(NIPAM-co-MAA)] and functionalized graphene oxide were confirmed by IR and Raman spectroscopy. Both the pH and temperature responsiveness in drug release from microcapsule was primarily confirmed by UV-illumination images and fluorescence microscopy. It was further confirmed using fluorescence spectroscopy and atomic absorption spectroscopy for cisplatin. MTT assay reveals that the synthesized polymer was highly biocompatible. The presence of the graphene sheets and surface morphology of polymeric microcapsules was confirmed by FESEM and HR-TEM analysis. The prepared microcapsules may be useful as carriers for site-specific delivery of hydrophilic drugs in human body. We are currently pursuing in that direction.

Acknowledgements We are grateful to the Department of Biotechnology (DBT), Government of India for the financial support through RGYI scheme (BT/PR6433/GBD/27/413/2012). The first author acknowledges the financial support from UGC through fellowship. Financial support from DST-INSPIRE Faculty Award (IFA13-CH130) is gratefully acknowledged. CSIR-CLRI communication No. A/2019/PLY/DST/1302.

Compliance with ethical standards

Conflict of interest There are no conflicts of interest to declare. All the authors' consent has been taken.

References

1. Chang CC, Letteri R, Hayward RC, Emrick T (2015) Functional sulfobetaine polymers: synthesis and salt-responsive stabilization of oil-in-water droplets. Macromolecules 48:7843–7850
2. Wei J, Ju XJ, Zou XY, Xie R, Wang W, Liu YM, Chu LY (2014) Multistimuli- responsive microcapsules for adjustable controlled-release. Adv Funct Mater 24:3312–3323
3. Bedard MF, De Geest BG, Skirtach AG, Mohwald H, Sukhorukov GB (2010) Polymeric microcapsules with light responsive properties for encapsulation and release. Adv Colloid Interface Sci 158:2–14
4. Gao H, Wen DS, Tarakina NV, Liang JR, Bushby AJ, Sukhorukov GB (2016) Bifunctional ultraviolet/ultrasound responsive composite TiO2/polyelectrolyte microcapsules. Nanoscale 8:5170–5180
5. Abbaspourrad A, Datta SS, Weitz DA (2013) Controlling release from pH-responsive microcapsules. Langmuir 29:12697–12702
6. Angelatos AS, Radt B, Caruso F (2005) Light-responsive polyelectrolyte/gold nanoparticle microcapsules. J Phys Chem B 109:3071–3076
7. Bi HM, Ma SH, Li QC, Han XJ (2016) Magnetically triggered drug release from biocompatible microcapsules for potential cancer therapeutics. J Mater Chem B 4:3269–3277
8. Li ZF, Liu SF, Wang SR, Qiang LH, Yang T, Wang HY, Mohwald H, Cui XJ (2015) Synthesis of folic acid functionalized redox-responsive magnetic proteinous microcapsules for targeted drug delivery. J Colloid Interface Sci 450:325–331
9. Ma YJ, Dong WF, Hempenius MA, Mohwald H, Vancso GJ (2006) Redox-controlled molecular permeability of composite-wall microcapsules. Nat Mater 5:724–729
10. Dong LL, Shi C, Guo LL, Yang T, Sun YX, Cui XJ (2017) Fabrication of redox and pH dual-responsive magnetic graphene oxide microcapsules via sonochemical method. Ultrason Sonochem 36:437–445
11. Zeng J, Du PC, Liu L, Li JG, Tian K, Jia X, Zhao XB, Liu P (2015) Superparamagnetic Reduction/pH/Temperature multistimuli-responsive nanoparticles for targeted and controlled antitumor drug delivery. Mol Pharm 12:4188–4199
12. Zhang K, Wu XY (2004) Temperature and pH-responsive polymeric composite membranes for controlled delivery of proteins and peptides. Biomaterials 25:5281–5291
13. Horecha M, Senkovskyy V, Stamm M, Kiriy A (2009) One-pot synthesis of thermoresponsive PNIPAM hydrogel microcapsules designed to function in apolar media. Macromolecules 42:5811–5817
14. Samanta D, Sawoo S, Patra S, Ray M, Salmain M, Sarkar A (2005) Synthesis of hydrophilic fischer carbene complexes as organometallic marker and PEGylating agent for proteins. J Organomet Chem 690:5581–5590
15. Schmaljohann D (2006) Thermo- and pH-responsive polymers in drug delivery. Adv Drug Deliv Rev 58:1655–1670
16. Dao TD, Jeong HM (2015) Novel stearic acid/graphene core shell composite microcapsule as a phase change material exhibiting high shape stability and performance. Sol Energy Mater Sol Cells 137:227–234
17. Zheng Z, Jin J, Xu G-K, Zou J, Wais U, Beckett A, Heil T, Higgins S, Guan L, Wang Y, Shchukin D (2016) Highly stable and conductive microcapsules for enhancement of joule heating performance. ACS Nano 10:4695–4703
18. Pentela N, Ayyappan VG, Krishnamurthy M, Boopathi AA, Rainu S, Sampath S, Mandal AB, Samanta D (2017) A comparative study of pH-responsive microcapsules from different nanocomposites. Green Mater 5:53–62
19. Silva KCG, Cezarino EC, Michelon M, Sato ACK (2018) Symbiotic microencapsulation to enhance *Lactobacillus acidophilus* survival. LWT Food Sci Technol 89:503–509
20. Wang XM, Gu JY, Tian L, Zhang X (2017) Hierarchical porous interlocked polymeric microcapsules: sulfonic acid functionalization as acid catalysts. Sci Rep 7:44178
21. Zhao X, Cao M, Liu B, Tian Y, Hu C (2012) Interconnected core-shell MoO2 microcapsules with nanorod-assembled shells as high-performance lithium-ion battery anodes. J Mater Chem 22:13334–13340
22. Ebdon JR, Huckerby TN, Hunter TC (1994) Free-radical aqueous slurry polymerizations of acrylonitrile: 1. End-groups and other minor structures in polyacrylonitriles initiated by ammonium persulfate/sodium metabisulfite. Polymer 35:250–256
23. Rodriguez F, Givey RD (1961) Polymerization of acrylamide with persulfate and metabisulfite initiator. J Polym Sci 55:713–719
24. Srinivasan S, Shin WH, Choi JW, Coskun A (2013) A bifunctional approach for the preparation of graphene and ionic liquid-based hybrid gels. J Mater Chem A 1:43–48
25. Cai DY, Song M (2007) Preparation of fully exfoliated graphite oxide nanoplatelets in organic solvents. J Mater Chem 17:3678–3680
26. Dikin DA, Stankovich S, Zimney EJ, Piner RD, Dommett GHB, Evmenenko G, Nguyen ST, Ruoff RS (2007) Preparation and characterization of graphene oxide paper. Nature 448:457–460
27. Hummers WS, Offeman RE (1958) Preparation of graphitic oxide. J Am Chem Soc 80:1339–1339
28. Srinivasan S, Je SH, Back S, Barin G, Buyukcakir O, Guliyev R, Jung Y, Coskun A (2014) Ordered supramolecular gels based on graphene oxide and tetracationic cyclophanes. Adv Mater 26:2725–2729
29. Sousa RG, Magalhaes WF, Freitas RFS (1998) Glass transition and thermal stability of poly(N-isopropylacrylamide) gels and some of their copolymers with acrylamide. Polym Degrad Stabil 61:275–281
30. Zhang J, Peppas NA (2000) Synthesis and characterization of pH- and temperature- sensitive poly(methacrylic acid)/poly(*N*-isopropylacrylamide) interpenetrating polymeric networks. Macromolecules 33:102–107
31. Schonhoff M, Larsson A, Welzel PB, Kuckling D (2002) Thermoreversible polymers adsorbed to colloidal silica: a H-1 NMR and DSC study of the phase transition in confined geometry. J Phys Chem B 106:7800–7808